

MODELING OF GEOGRID REINFORCED EMBANKMENTS FOR ROCKFALL PROTECTION

A. Carotti, C. Di Prisco, M. Vecchiotti

Dept. Structural Eng.- Politecnico di Milano Tech. University, Milano, Italy

P. Recalcati

TENAX SpA – Geosynthetics Technical Office, Milano, Italy

P. Rimoldi

World Tech Engineering Srl, Milano, Italy

ABSTRACT: Geogrid reinforced embankments find more and more applications as barriers against rocks fall, for the protection of all kind of infrastructures. Mathematical models of reinforced soil structures subject to dynamic impacts have been developed, based on ballistic, structural mechanics and soil mechanics principles. In this paper the Authors wish to present the state of the art in this peculiar field: from early models derived from experiments on totally different kind of structures, to a model based on anelastic impact principles, to a rheological model which takes into account the phase of impact, where only local phenomena are encountered, and the phase of subsequent motion of a soil mass triggered by the energy exchange between the impacting boulder and the barrier. The paper presents the latest advancements in the modeling of such complex structures, and preludes to a systematic research aimed at defining the design methods for reinforced soil barriers for rockfall protection.

1 INTRODUCTION

Rock fall protection reinforced soil structures feature high energy absorption, to deal both with high energy impacts and with “swarms” of falling boulders. For the design of reinforced soil rock-fall protection walls and embankments, it is important to afford a mathematical model able to provide, easily and quickly, the order of magnitude of forces and deformations due to a given impact.

Mathematical models of reinforced soil structures subject to dynamic impacts have been developed, based on ballistic, structural mechanics and soil mechanics principles. In this paper the Authors wish to present the state of the art in this peculiar field.

2 EARLY MODELS

Very rough methods are present in bibliography, which can be used for a first evaluation of the behaviour of a soil rockfall passive barrier. As the evaluation of the effect of the impact of a block having high kinetic energy on a soil structure is extremely complex, defining the energy dissipation mechanism and the collapse mechanism through a close form equation is an operation that may require sometimes unacceptable approximations.

The collapse mechanism that has to be taken into account is for sure the rock block passing through the structure; according to this failure mechanism the thickness of the barrier in the impact point seems to be a very important parameter.

Overturing of the structure doesn't seem to be a sensible failure mechanism, also taking into account the important downward vertical component of the block speed; in certain cases also a structural collapse due to excessive deformation of the barrier after the impact can be considered as realistic.

The first type of close form equation used to evaluate the behaviour of a soil barrier as a rock fall passive protection system has been proposed by Kar (1978).

This method is based on ballistic principles and derives from true scale tests performed to evaluate the penetration depth of bombs and missiles on soil protection shelter structures; it is characterised by a series of empirical equa-

tions whose result is mainly the expected depth Z in the impact area:

$$Z = \frac{27183}{\sqrt{Y}} \cdot N \cdot \left(\frac{E}{E_s} \right)^{1.25} \cdot \frac{m}{d^{2.31}} \cdot \left(\frac{V}{1000} \right)^{1.25} \quad (1)$$

Where:

- E (kPa) is the elastic modulus of the impacting block;
- E_s (kPa) is the elastic modulus of the steel (tests have been conducted with missiles);
- m (kg) is the block mass;
- d (cm) is the impact dimension;
- V (m/sec) is the block speed;
- N is a shape coefficient;
- Y is the unconfined compressive resistance.

The main problem of this method, apart from applying a ballistic method to a soil structure whose function is to act as a barrier, is given by the fact that, among the required values, the only one that characterises the soil barrier is the unconfined elastic modulus. If it is easy to evaluate this modulus for a rock or for a cohesive material in undrained condition (for example through unconfined compressive tests), it is almost impossible to determine the same value for a frictional material.

Since almost all the rockfall barriers are made of a frictional soil, hence the method gives values that can be dramatically wrong, just for the difficulty to use the proper design values.

Another approach allows to determine the maximum force F_{max} applied to the centre of mass of the block (and the maximum deceleration), and to determine the maximum penetration d applying the principle of conservation of the momentum.

If we assume that the deceleration of the block occurs during the time elapsed from the instant when the block touches the barrier and the instant when it is stopped, and we also assume that the impact force passes from the maximum value to zero during the same elapsed time, the work made by the impact force can be calculated as:

$$F_{medium} \cdot d = \frac{1}{2} \cdot F_{max} \cdot d \quad (2)$$

As the work done by the impact force is equal to the kinetic energy dissipation, we can write

$$\frac{1}{2} \cdot F_{\max} \cdot d = \frac{1}{2} \cdot m \cdot v^2 \quad (3)$$

and finally

$$d = \frac{m \cdot v^2}{F} \quad (4)$$

where m is the block mass, v is the block speed and F is the force applied to the centre of mass.

To evaluate the maximum force it is possible to use the formula proposed by Montani et al. (1996). This formula, however, has been used to evaluate the impact of rock blocks falling over the protection cover system of artificial tunnels: again it is not describing the real situation. According to this approach, the maximum force can be calculated as

$$F_{\max} = 1.765 \cdot M_E^{2/5} R^{1/5} W^{3/5} H^{3/5} \quad (5)$$

where M_E is the elastic modulus of the soil (it can be determined as E_{V1} from a plate bearing test), R is the curvature radius of the impact block (assumed as spherical), W is the block weight and H is the fall height.

Another possibility to evaluate F_{\max} derives from a correlation proposed by Mayne et al. (1983) that derives from heavy tamping soil consolidation experience:

$$F_{\max} = \sqrt{\frac{32 \cdot W \cdot H \cdot G \cdot r_0}{\pi^2(1-\nu)}} \quad (6)$$

where W is the block weight, r_0 is rock block radius, H is the rock fall height, ν is Poisson coefficient and G is the soil shear modulus.

Comparing the results derived from true scale tests with the values obtained with the equations above, it is possible to notice how Kar method overestimates the depth, while the other methods underestimate it (Recalcati et al., 2001).

The lower depth and the much higher forces obtained through Montani or Mayne approaches derive from the greater rigidity of the elastic half-space in respect to the real structure, which has a finite shape, is not elastic and can be subjected to relative displacements between reinforced layers.

Table 1 Comparison between calculated and experimental results

Model	Depth [mm]	Fmax [kN]
Kar	1170	2306
Montani et al.	130	22160
Mayne et al.	220	11742
Real test	700	-

3 ANELASTIC IMPACT MODEL

More realistic results can be achieved through a mathematical model based on the physics of anelastic impact phenomena.

According to the theorem of Carnot, during an anelastic impact part of the kinetic energy of the colliding bodies is lost. The larger loss occurs for a perfectly anelastic impact, that is when the two colliding bodies completely melt into a new entity. Let's calculate the loss of kinetic energy during an anelastic impact between two bodies. Let's suppose that the two body have translational motion; indicating with u their common velocity after a perfectly anelastic

impact, the kinetic energy before and after the impact is given by:

$$K_0 = \frac{1}{2} (M_1 v_{1x}^2 + M_2 v_{2x}^2) \quad (7)$$

$$K_1 = \frac{1}{2} (M_1 + M_2) u_x^2 \quad (8)$$

The loss of kinetic energy is equal to $K_0 - K_1$.

After mathematical development of Eq. 7 and 8, we obtain:

$$K_0 - K_1 = \frac{1}{2} M_1 (v_{1x} - u_x)^2 + \frac{1}{2} M_2 (v_{2x} - u_x)^2 \quad (9)$$

The differences $(v_{1x} - u_x)$ and $(v_{2x} - u_x)$ show how much the velocity of the two colliding bodies has decreased. We can call them lost velocities during the impact. Then from Eq. 9 derives the following theorem of Carnot: the kinetic energy lost by the system of the two colliding bodies during a perfectly anelastic impact is equal to the kinetic energy that the system would have if the two bodies move with the lost velocities.

In case of anelastic impact against a firm body, it is $v_2 = 0$ and:

$$K_0 = \frac{1}{2} M_1 v_1^2 \quad (10)$$

$$u = \frac{M_1 v_1}{M_1 + M_2} \quad (11)$$

$$K_1 = \frac{M_1}{M_1 + M_2} K_0 \quad (12)$$

When the mass of the impacted body is far larger than the mass of the impacting body ($M_2 \gg M_1$), we can write:

$$\frac{M_1}{M_1 + M_2} \approx 0 \quad (13)$$

In this case Eq. 12 gives: $K_1 \approx 0$.

Therefore during the impact almost all the kinetic energy is spent for deforming the colliding bodies; at the end of impact the two bodies can be considered as firm.

If the impact is not perfectly anelastic ($k = u / v \neq 0$), from similar considerations we obtain the loss of kinetic energy during the impact:

$$K_0 - K_1 = \frac{1-k}{1+k} \left[\frac{1}{2} M_1 (v_{1x} - u_{1x})^2 + \frac{1}{2} M_2 (v_{2x} - u_{2x})^2 \right] \quad (14)$$

The common speed after impact is still given by Eq. 11.

Let's make now reference to structures with vertical or sub-vertical front and back faces, with horizontal reinforcements (see Figure 1), subject to the impact of a spherical block having velocity with both downward vertical component and horizontal component. Let's also suppose that the impact, beside the deformation of the barrier, produces a rigid rotation of the reinforced soil structure, as it can be seen in the same Figure 1.

In such case the centre of rotation is moved downward in respect to the impact area, due to the vertical component of the block speed and to the stiffness of the face.

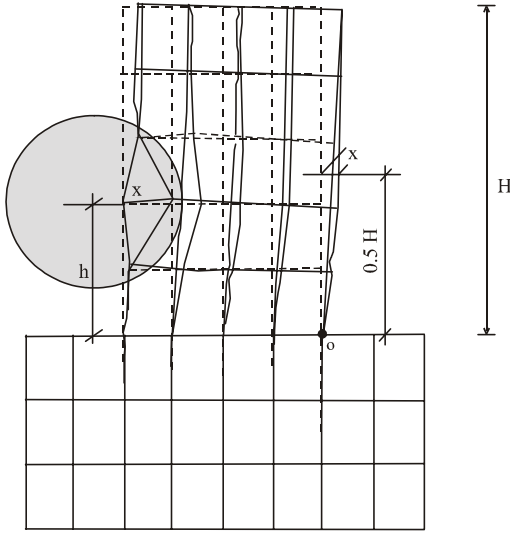


Figure 1 Scheme of the structure used for the anelastic impact model (from Borroughs et Al, 1993)

The “angular momentum” of the boulder-soil system before (suffix “b”) the impact is:

$$\Gamma_{0_b} = (m_r \cdot v_r) \cdot h \quad (15)$$

while after (suffix “a”) the impact it becomes:

$$\Gamma_{0_a} = (m_r \cdot v) \cdot h + \frac{m_w H^2}{3} \omega \quad (16)$$

where:

- h distance between the centre of gravity of the boulder and the centre of rotation;
- H height of soil above the centre of rotation;
- ω angular velocity of the boulder-wall system;
- m_r , m_w mass of the rock and of the wall;
- v_r velocity of the rock.

Since there is no other external action during the impulse except gravity (whose static moment is not significantly large during the impulse), it must be:

$$\Gamma_{0_b} = \Gamma_{0_a} \quad (17)$$

or

$$h m_r \cdot v + m_w \frac{H^2}{3} \omega = m_r v_r \cdot h \quad (18)$$

Given that the collision is totally anelastic, the boulder is captured by the soil structure, resulting in a velocity

$$v = \omega \cdot h \quad (19)$$

Then Eq. (18) becomes:

$$\omega = \frac{m_r \cdot h \cdot v_r}{\left(h^2 m_r + m_w \cdot \frac{H^2}{3} \right)} \quad (20)$$

Since:

$$K_1 = \frac{1}{2} I_0 \cdot \omega^2 \quad (21)$$

with:

$$I_0 = m_r h^2 + m_w \cdot \frac{H^2}{3} \quad (22)$$

Then Eqs. (20)-(22) allow to calculate ω.

The total work dissipated in a rotation $d\vartheta$ of the system is:

$$L = M_0 \cdot d\vartheta = \sum_1^n F_i b_i d\vartheta \quad (23)$$

with

- M_0 initial moment;
- F_i tensile force in the i -th reinforcement layer;
- b_i arm of the i -th reinforcement layer from the centre of rotation.

By imposing the balance equation:

$$L = K_1 \quad (24)$$

the rigid rotation $d\vartheta$ can be calculated, and therefore also the related rigid displacement

$$x_{\text{rigid}} = z d\vartheta \quad (25)$$

at any elevation z above the centre of rotation.

The duration dt_{rigid} of the rigid rotation can be easily calculated as well:

$$dt_{\text{rigid}} = \frac{d\vartheta}{\omega} \quad (26)$$

The motion of the system is arrested when the residual energy K_1 equals the work dissipated by the coulombian friction between the soil and the reinforcement layers.

The shear stress of the soil-reinforcement interface is:

$$\tau = \sigma_v \tan \varphi \cdot f_{ds} \quad (27)$$

where:

- σ_v vertical stress in the soil at the considered elevation;
- φ peak friction angle of the soil;
- f_{ds} direct shear coefficient

The shear force at the i -th soil-reinforcement interface is therefore:

$$F_i = \tau_i \cdot A_i \quad (28)$$

where:

- A_i area of reinforcement affected by the motion due to the impact.

As a first hypothesis, we can suppose that the soil mass and the reinforcement layers involved in the motion activated by the impact, and therefore “collaborating”, have the extensions shown in Figure 2.

For a dynamic analysis of the motion of this collaborating system, we can characterize the soil with (Carotti & Rimoldi, 1997):

- a horizontal stiffness coefficient K ;
- a viscous damping coefficient C ;
- a Coulomb friction force F_c .

We can also characterize the reinforcing layers with (Carotti & Rimoldi, 1997):

- a horizontal stiffness coefficient K_{gg} ;
- a viscous damping coefficient C_{gg} .

These parameters in reality act in the cone limited by the angle α in Figure 2b. With a further approximation, we can suppose that they act along the external surface of this cone. Then their component along the impact direction, supposed normal to the face, is:

$$K_n = K \cdot \cos^2 \alpha \quad (29)$$

and similarly for the other coefficients.

Then the collaborating soil-reinforcement system can be reduced to an equivalent 1-DOF oscillator, as shown in Figure 2 and 3.

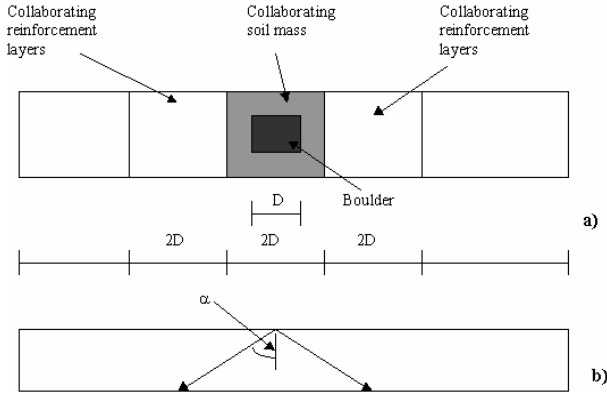


Figure 2 First hypothesis of collaborating soil mass and reinforcement layers: a) front view; b) plan view.

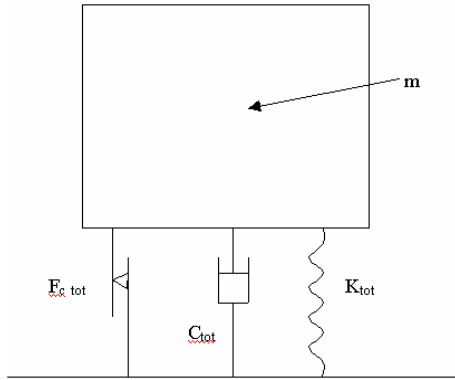


Figure 3 Equivalent 1-DOF oscillator

$$K_{tot} = K_n + K_{gg_n} \quad (30)$$

$$C_{tot} = C_n + C_{gg_n} \quad (31)$$

$$F_{e_{tot}} = F_{e_n} \quad (31)$$

The circular frequency of this oscillator is given by:

$$\omega = \sqrt{K_{tot}/m} \quad (33)$$

The impulse force F generated by the impact can be evaluated as follows:

$$I = m_1(k+1)v_1 = m_1v_1 \quad (34)$$

$$I = F \cdot dt \quad (35)$$

$$F = \frac{m_1v_1}{dt} \quad (36)$$

The viscous work (L_v) during a deformative cycle with maximum displacement x_d is equal to $1/4$ of the surface of the elliptical cycle in an ideal oscillation

$$L_v = \frac{1}{4} \cdot \pi \cdot C_{tot} \cdot \omega \cdot x_d \cdot x_d + F_{e_{tot}} \cdot x_d \quad (38)$$

Since it must be:

$$L_v = K_0 - K_1 \quad (39)$$

then it is possible to obtain x_d .

The total displacement of the reinforced soil structure at any elevation is finally:

$$x_{tot}(z) = x_{rigid}(z) + x_d(z) \quad (40)$$

4 RHEOLOGICAL MODEL

An alternative approach in the design of embankments for rock fall protection has been recently proposed by two of the authors (di Prisco and Vecchiotti 2003). The model interprets the impact phenomenon by analysing separately the local response to the impact and the failure mechanism involving the protection structure. This implies a two stage approach:

1. Evaluation of the forces involved in the local impact phenomenon (maximum force transmitted by the boulder to the embankment);
2. Estimation of the displacements of the material involved in the failure mechanism.

The first task can be accomplished either numerically (by performing 3D FEM analyses) or experimentally. As far as the former method is concerned, it is well known that many difficulties make the obtained results dramatically dependent both on the chosen numerical algorithm and on the introduced constitutive model for the soil. An alternative and promising numerical approach consists in performing DEM (Distinct Element Method) analyses. In this case, the soil layer is described as the assembly of a large number of grain particles. The penetration of the boulder can be described even if the local displacements are very large. On the contrary, as far as the experimental approach is concerned, a large number of empirical relationships can be found in literature, like those proposed by Labiouse *et al.* (1994), based on the experimental tests performed at the EPFL's labs of Lausanne. Even if the experimental apparatus employed in these tests was originally designed to investigate rock-fall loads on shelters, very important data have been collected about inertial forces acting on the structure and about the displacement of the boulder penetrating in the soil cushion. Unfortunately, these tests concerned only vertical impacts on horizontal soil strata and the maximum boulder's energy taken into consideration is too low with respect to real cases.

Very recently, Calvetti (1998) simulated numerically the Labiouse's experimental data by using the UDEC code (Itasca). In Figure 4, jointly to the experimental set-up employed by Labiouse *et al.* (1994), a comparison between recorded data and numerical simulations is illustrated. A crucial problem concerning the use of such an approach as a design tool consists in the calibration of the constitutive parameters describing the interfaces among grains.

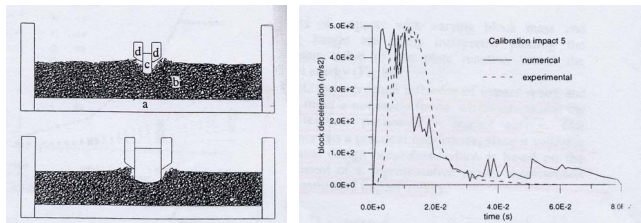


Figure 4 DEM model and numerical results from Calvetti (1998)

In order to simplify the analysis of the local response of the soil to the impacting boulder, two of the authors recently developed a rheological model (Nova and di Prisco, 2003; di Prisco and Vecchiotti, 2003), capable of reproducing satisfactorily both the impact forces and the rock trajectory after the impact.

The model is based on the following main hypotheses:

- the rock, spherically shaped, can be modelled as a shallow circular foundation, whose radius increases during the impact up to R (boulder radius);
- the rock and the granular soil subject to impact are assumed to be a macro-element (Nova and Montrasio, 1991), characterised by an elasto-visco-plastic strain hardening constitutive relationship, with a non-associate flow rule.

The macro-element concept cited above assumes the presence of a rigid element (in our case the rock boulder) whose kinematics description is fulfilled by a vector with four components, which four generalised forces are associated to. For the sake of simplicity, in the model proposed by the authors the trajectory of the boulder is assumed to be planar and rotations are neglected. As a consequence, the vectors describing generalised displacements \underline{q} and the associated generalised forces \underline{Q} are two-dimensional. As far as vertical impacts are concerned, we can schematically sketch the model as shown in Figure 5.a; where it is easy to recognise an elastic spring, a viscous damper and a viscoplastic slider. This latter is described by the viscoplastic flow rule (Perzyna, 1963) defined here below:

$$\dot{q}^{vp} = \phi(f) \frac{\partial g}{\partial Q} \quad (41)$$

where f and g are the yield function and the plastic potential, respectively. For the sake of simplicity, the viscous nucleus has been defined as $\phi = \langle \gamma d + c \rangle$, where the brackets imply that the reported definition is valid only for positive values of their content, whereas for negative values $\phi = 0$. In this latter definition γ and c are constitutive parameters while d is the distance between the point corresponding to the generalised stress state \underline{Q} and the associated image point on the yield function defined by means of a radial mapping rule (Figure 5.b). As is evident from Figure 5.b, such an operation is done in the nondimensional space ξ, h ($\xi = V/V_{max}$ and $h = H/\mu V_{max}$, where V_{max} is the bearing capacity of the pseudo-foundation under centred vertical loading while μ is a constitutive parameter defining the horizontal sliding). The most of the parameters requested by the model is related to common geotechnical data like the internal friction angle Φ' , the Young's modulus E and the relative density D_r ; only γ and c need to be calibrated on *ad hoc* experimental data.

Despite of its simplicity, the model performances are encouraging: in Figure 6 experimental data from Labiouse *et al.* (1994), concerning a mass of 100 kg falling from an height of 10 m on a gravel-like cushion, are compared with the aforementioned model predictions. It is important to underline that in Figure 6.a,b,c the calibration curves are illustrated, whereas in Figure 6.d the validation ones. We must underline that each numerical curve corresponding with a certain mass is characterised by a unique set of constitutive parameters. By changing the mass of the boulder, we are forced to change the values of γ and c . This is physically meaningful because the change in the boulder mass is associated to a change in the boulder radius and consequently in the failure mechanism size.

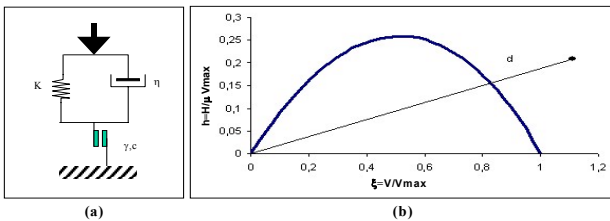


Figure 5 - (a) Model structure, (b) failure locus (from Nova and Montrasio, 1991)

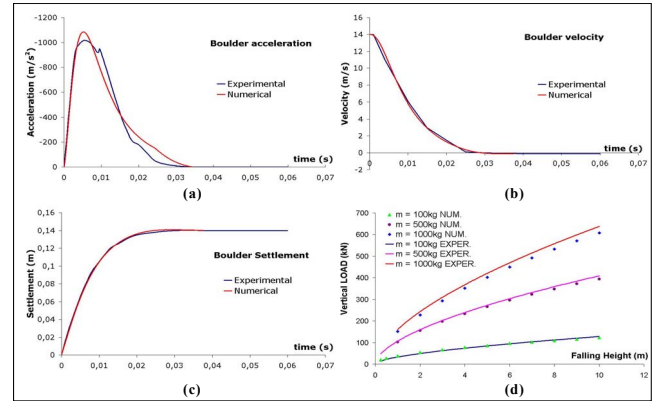


Figure 6 Comparison between numerical and experimental data

The model allows the engineer to analyse not only vertical impacts on horizontal surfaces but even inclined impacts on inclined slopes. In Figure 7, for instance, the trajectory of a boulder during the impact on a slope inclined of 63° (the presence of geosynthetics reinforcements make possible such an angle of slope inclination) is illustrated. This makes such an approach available for analysing the dynamic local failure mechanism due to the impact of a rock boulder on a reinforced embankment.

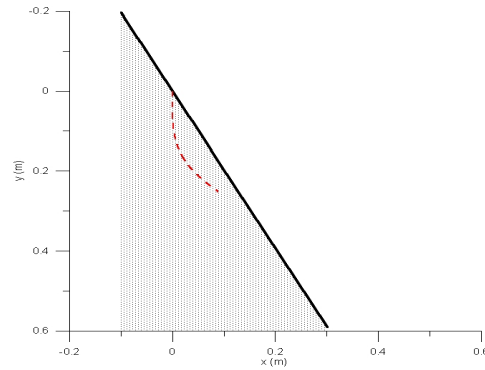


Figure 7 Boulder's trajectory on a slope inclined of 63°

The second task consists in describing the evolution of the failure mechanism within the embankment. In this case, the whole geometry cannot be disregarded. As is sketched in Figure 8, where the complete system is represented, a further degree of freedom is introduced: m_1 stands for the boulder mass, while m_2 stands for the mass of the soil belonging to the embankment involved in the global failure mechanism (Figure 9). In this case, the dashpot is assumed to be perfectly plastic. Obviously, for the sake of brevity a one dimensional system is illustrated while the real model is geometrically two dimensional.

In order to evaluate the resistance force, a large number of 2D and 3D failure analyses were carried out by means of both the limit equilibrium method and a FEM code (Tochnog, Roddeman, 2000). The presence of geosynthetics was considered by disregarding the effects due to large displacements. The resistance force value F_{CR} is a function of the embankment geometry, of the impact point position s and of the boulder trajectory described by the aforementioned local model (Figure 10).

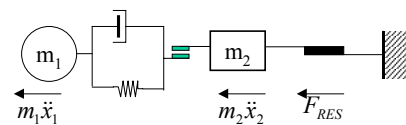


Figure 8: Dynamic of the embankment subject to global failure

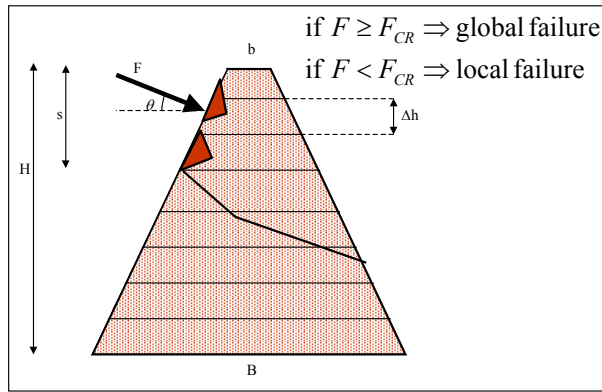


Figure 9: Local and global failure mechanisms

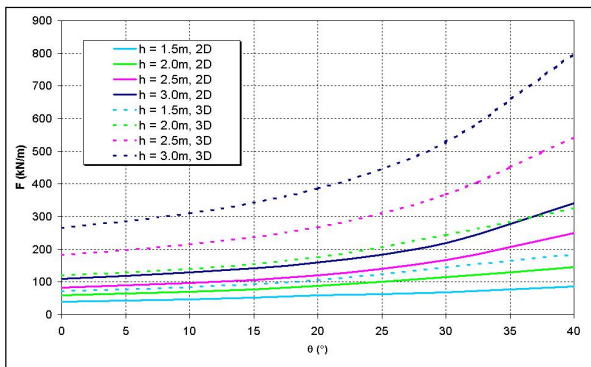


Figure 10: Example of computed values for F_{CR}

If the condition $F > F_{CR}$ is satisfied, global collapsing occurs and the mass m_2 of the global failure mechanism starts moving, causing irreversible damage of the embankment. As is exemplified in Figure 11, the impact phenomenon becomes therefore the sequence of three distinct phases:

- Phase number 1 (the local phenomenon), during which $\dot{x}_1 > 0$ and $\dot{x}_2 = 0$. In fact, the force acting on m_2 is less than F_{CR} .
- Phase number 2 (the transition condition), during which $\dot{x}_1 > 0$ and $\dot{x}_2 > 0$ but $\dot{x}_1 \neq \dot{x}_2$. The boulder continues in penetrating within the embankment, even if a global mechanism is activated.
- Phase number 3 (the global failure phenomenon) during which $\dot{x}_1 = \dot{x}_2 > 0$. The boulder translates together with the soil block defined by the 3D sliding surface.

The type and duration of the three phases depend on many factors regarding the impact energy and the embankment structure.

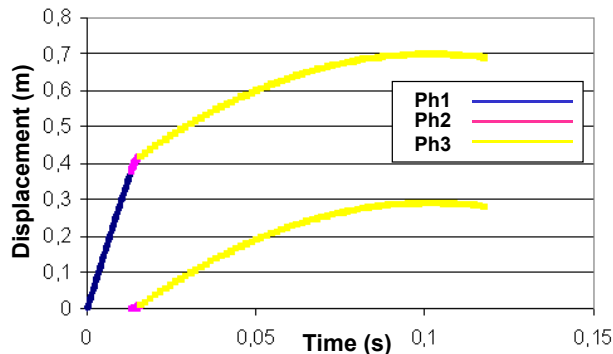


Figure 11: Description of the impact phenomenon

5 CONCLUSIONS.

Mathematical models of reinforced soil structures subject to dynamic impacts have been developed, based on ballistic, structural mechanics and soil mechanics principles. From early models derived from experiments on totally different kind of structures, research has advanced to a model based on anelastic impact principles and to a rheological model which takes into account the phase of impact, where only local phenomena are encountered, and the phase of subsequent motion of a soil mass triggered by the energy exchange between the impacting boulder and the barrier. The work is just started, but the methods illustrated in the present paper seems very promising and they will allow in the near future to yield proper design methods for reinforced soil rock fall protection structures.

6 REFERENCES.

- Burroughs D.K., Henson H.H. e Jiang S.S. , (1993), *Full scale geotextile rock barrier wall testing, analysis and prediction*, Geosynthetics 1993, Vancouver: 959-970.
- Calveti F. (1998), *Distinct element evaluation of the rock fall design loads for shelters*, Rivista Italiana di Geotecnica, 3, pp. 63-83
- Carotti A. e Rimoldi P. ,(1998), *Parametric study for geosynthetic reinforced walls under sustained earthquakes*, Sixth International Conference on Geosynthetics, Atlanta, Georgia (USA): 25-29.
- Di Prisco C., Vecchiotti M. (2003), *Impatti di blocchi in roccia su rilevati in terra: analisi numeriche e modellazione teorica*, XVI Convegno Nazionale "Geosintetici nelle costruzioni in terra: costruzioni marittime ed interventi in ambiente montano", Ottobre 2003, Bologna (SAIE2003)
- Labrousse V., Descedreuses F., Montani S., Schmidhalter C.-A. (1994), *Etude experimentale de la chute de blocs rocheux sur une dalle en beton arme recouverte per des materiaux amortissants*, Review Francaise de Geotechnique, 69, 4, pp. 41 – 62
- Nova R., di Prisco C. (2003), *The macro-element concept and its application in geotechnical engineering*, FONDSUP2003 Int. Symp.
- Nova R., Montrasio L. (1991), *Settlements of shallow foundations on sand*, Geotechnique, 41, No.2
- Perzyna P. (1963), *The constitutive equations for rate sensitive plastic materials*, Quart. Appl. Math., vol. 20
- Recalcati, P, Castiglia, C, Oggeri, C. (2001) *Linee progettuali per rilevati paramassi*, Conference on rockfall protection, Siusi (BZ), Italy.
- Roddeman D. (2000), *TOCHNOG User's manual – a free explicit/implicit FE program*, from the web site <http://tochnog.sourceforge.net/>